enough to enable the estimation of $(PO)_3$. This domain should not extend to infinity as four-impulse trajectories are necessary when $\phi > 4\pi$ and optimal when $\tau \to \infty$. A complete computation of $(PO)_3$ and $(PO)_4$ is called for to ascertain whether or not four impulses are sufficient in the nonlinear case.[15] Such are the questions left open about impulsive rendezvous, to say nothing of the uniqueness of the solutions found, which, in spite of the present results, can be questioned.[7]

References

[1] Lambert, J. H., *Insignores Orbitae Cometarum Proprietates*, Monograph, 1761, W. Engelmann, Leipzig, East Germany, 1902.

[2] Breakwell, J. V., Gillespie, R. W., and Ross, S., "Researches in Interplanetary Transfers," *ARS Journal*, Vol. 31, No. 2, Feb. 1961, pp. 201–208.

[3] Jordan, J. F., "The Applications of Lambert's Theorem to the Solution of Interplanetary Transfer Problems," TR 35.521, Feb. 1, 1964, Jet Propulsion Lab., Pasadena, Calif.

[4] Pines, S., "A Uniform Solution of Lambert's Problem," Internal Note 65 FM 166, Dec. 13, 1965, Manned Spacecraft Center, Houston, Texas.

[5] Battin, R. H., "A New Solution for Lambert's Problem," *Proceedings of the XIXth International Astronautical Congress*, Vol. 2, Pergamon, New York, 1970, pp. 131–150.

[6] Lawden, D. F., *Optimal Trajectories for Space Navigation*, Butterworths, London, 1963; also "Fundamentals of Space Navigation," *Journal of the British Interplanetary Society*, Vol. 13, No. 2, 1954, pp. 87–101.

[7] Peltier, J. P., "Étude numérique de l'optimalité des rendezvous bi-impulsionnels entre orbites planétaires (circulaires et coplanaires)," *La Recherche Aérospatiale*, No. 6, Nov.–Dec. 1970, pp. 291–300.

[8] Handelsman, M., "Some Necessary Conditions for Optimal Fixed-Time Powered Transfers with Multiple Coast and Thrust Between Circular Orbits," *Proceedings of the XVIIth I.A.F. Congress*, Madrid, Spain, Oct. 1966.

[9] Lion, P. M. and Handelsman, M., "The Primer Vector on Fixed Time Impulsive Trajectories," *AIAA Journal*, Vol. 6, No. 1, Jan. 1968, pp. 127–132.

[10] Prussing, J. E., "Optimal Four-Impulse Fixed-Time Rendezvous in the Vicinity of a Circular Orbit," *AIAA Journal*, Vol. 7, No. 5, May 1969, pp. 928–935.

[11] Prussing, J. E., "Optimal Two- and Three-Impulse Fixed-Time Rendezvous in the Vicinity of a Circular Orbit," *AIAA Journal*, Vol. 8, No. 7, July 1970, p. 1221.

[12] Marec, J. P., "Rendez-vous multi-impulsionnels, optimaux, de durê moyenne, entre orbites quasi-circulaires, proches, coplanaires," *Proceedings of the XIXth International Astronautical Congress*, Vol. 2, Pergamon Press, New York, 1970, pp. 173–200.

[13] Peltier, J. P., "Investigation about some Impulsive Trajectories for Optimal Rendezvous," AMS Rept. 916c, July 1970, Aerospace Systems Lab., Princeton Univ., Princeton, N.J.

[14] Minkoff, M. and Lion, P. M., "Optimal Multi-Impulse Rendezvous Between Trajectories," *Proceedings of the XIXth International Astronautical Federation Congress*, New York, Oct. 1968.

[15] Edelbaum, T. N., "How many Impulses?," *Astronautics and Aeronautics*, Vol. 5, No. 11, 1967, pp. 64–69.

APRIL 1972 AIAA JOURNAL VOL. 10, NO. 4

Orbital Eccentricity and Angular Momentum Management Scheme Stability

RONALD A. MAYO*

The Bendix Corporation, Navigation and Control Division, Denver, Colo.

The class of angular momentum management schemes considered in this paper consists of a large attitude maneuver followed by a sequence of trim maneuvers. The characteristic equation is derived for general momentum sampling, switching logic, and system gains. The satellite orbital parameters are assumed arbitrary and in the neighborhood of the reference orbit. For a specific sampling scheme, the sampled momentum by the *n*th orbit is shown to converge to the sum of the classical Neumann series on momentum space augmented by the initial CMG cluster momentum. For small eccentricity, a linear (first order in eccentricity) management scheme stability analysis is presented. These studies are combined in a derivation of the range of eccentricity for which the continuous time CMG momentum remains bounded within the saturation limit of the momentum exchange device for arbitrary angular position of perigee. The results are extended to allow variation in the mean orbital radius.

Nomenclature

$K(a, \varepsilon, \theta_p)$	= linear operator on momentum space
$g(a, \varepsilon, \theta_p)$	= disturbance momentum accumulation per orbit after first orbit; sampling scheme (2)
$\tilde{g}(a, \varepsilon, \theta_p)$	= disturbance momentum accumulation for first orbit only; sampling scheme (2)
$(a, \varepsilon, \theta_p)$	= true orbital parameters
A, B, C	= control functions (switching logic and system gains) dependent on θ
θ	= angular position of vehicle in orbital plane with respect to $\hat{X}_R$
g_0	= acceleration of gravity at R_0
R_0	= mean radius of Earth
r	= distance from Earth's center to center of mass of vehicle
$\hat{r}$	= unit vector directed from center of Earth to center of mass of vehicle
I	= inertia tensor of vehicle
$M_\theta, M_\varepsilon, M_0$ M_t, M_{cf}	= linear operators on momentum space
M_{jk}	= linear operator having representation with respect to $\hat{X}_v, \hat{Y}_v, \hat{Z}_v$ axes consisting of all zeros except (j, k) element which equals one
$\Phi(\theta)$	= transition matrix on momentum space
$F^*(z), C^*(z)$	= 3×3 transition matrices in z-transform domain
$Q(a, \varepsilon, \theta_p)$	= $\int M_\theta(dt/d\theta)d\theta$ linear operator on momentum space; $\int$ denotes integration on desaturation period $[(2n+1)\pi, 2(n+1\pi)$; $Q(a, \varepsilon, \theta_p)$ is independent of n
$\tilde{\pi}$	= uncontrollable vector torque (independent of control functions) during desaturation period
$M_\theta H_0(2n\pi)$	= controllable vector torque (dependent on control functions) during desaturation period
$H_e(\theta)$	= error momentum; sum of disturbance momentum plus controllable vector momentum
$\oint$	= integration over complete orbit
$\hat{X}_R, \hat{Y}_R, \hat{Z}_R$	= ATM reference system (Fig. 1 and Fig. 2)
$\hat{X}_b, \hat{Y}_b, \hat{Z}_b$	= principal axes of satellite inertia tensor
$\hat{X}_v, \hat{Y}_v, \hat{Z}_v$	= vehicle axes; the principal axes are coincident with the vehicle axes only during experimental hold mode
$\lVert \cdot \rVert$	= the Euclidean norm on momentum space

Received July 6, 1971; revision received November 22, 1971.

Index categories: Manned Space Station Systems; Spacecraft Mission Studies and Economics; Spacecraft Attitude Dynamics and Control.

* Project Engineer, Guidance and Control Systems.

$\|\cdot\|_{op}$ = operator norm
M'_θ = defined by $M_\theta = (3g_0R_0^2/2r_0C_0)M'_\theta$
$\hat{X}_{bv}$, $\hat{Y}_{bv}$, $\hat{Z}_{bv}$ = body fixed vehicle axes (for simplicity this coordinate system is assumed coincident with the principal axes $\hat{X}_b$, $\hat{Y}_b$, $\hat{Z}_b$)
$\lim_q \uparrow \sup_{\theta, n<q} \|f_n(\theta)\|$ = lease upper bound on the Euclidean norm of the sequence of vector functions, f_n, on $0 \le \theta \le 2\pi$
q = index
τ = set of trajectories for which the sampled momentum remains bounded; derived in text
$H_0(\cdot)$ = vector output of digital controller
$H_{0j}(\cdot)$ = jth (x, y, or z) component of $H_0(\cdot)$
$*$ = convolution sign

I. Introduction

SKYLAB ATM experiments require an inertially-fixed (sun-oriented) satellite during the daylight portion of the orbit. Gravity gradient, aerodynamic, and solar radiation torques on the vehicle must be absorbed by a momentum exchange device which is a system of three double-gimbaled Control Moment Gyros (CMGs).[1,2] Because of the orbital eccentricity, the gravity gradient torque has a noncyclic component not only along the principal axis of the vehicle inertia tensor in the orbital plane but also along the remaining principal axes. This noncyclic component in the torque environment causes an average increase in the angular momentum stored in the CMG cluster. But the CMG cluster has only a limited momentum absorption capacity. Therefore, the cluster momentum must be managed by a policy that restricts the CMG momentum within the saturation limit throughout the mission.

Momentum management policies initiated during the nocturnal orbital sector, other than mass expulsion policies, rely on an adaptive sequence of large and small vehicle attitude maneuvers and on the consequences of the gravity gradient torque to insure that the attitude control system performs within the saturation limit of the CMG system. The adaptive sequence of attitude maneuvers depends on a momentum sampling scheme, switching logic, and suitable system (or management policy) gains.

The subject of Orbital Eccentricity and Angular Momentum Management Scheme Stability deals with the preservation under orbital perturbation of the attitude hold capability throughout the ATM experiments using gravity gradient momentum management. Angular momentum management schemes studied to date are dependent on the orbital parameters of the reference orbit. Moreover, simulation studies performed for Skylab A indicate that momentum management schemes may prove inadequate (e.g., the continuous time CMG momentum history may not remain within the saturation level of the momentum exchange system) for slight changes of the torque environment; in particular, for the addition of aerodynamic torques. In this study, the vehicle was constrained to the reference orbit. If the momentum management scheme is designed for the reference orbit and the space station's true orbit is an unknown perturbation of the reference orbit, not only is the torque environment slightly changed, but the momentum management scheme is no longer programed for the true orbital parameters.

Previous studies of momentum management restrict the vehicle to a circular reference orbit. In Refs. 3 and 4, convergence of the proposed schemes for a vehicle on the design orbit has not been proven. Another management policy proves stable only if the the gains are chosen to satisfy additional constraint equations.[5,6] In still another policy, gains are derived partially by trial and error so that simulated results are acceptable.[7] In all previous studies no stability analysis has been completed for satellite orbits in the neighborhood of the design orbit.[3–14]

This paper is concerned with momentum management scheme stability for satellite orbits in the neighborhood, η, of the design circular orbit. The management scheme is defined as stable over η if the sampled momentum remains bounded within H^0_{sat}, where

$$H^0_{sat} \triangleq H^{01}_{sat} - (1-\alpha)^{-1}M^0 \quad 0 < \alpha < 1 \tag{1}$$

and

$$M^0 = \sup_\tau \lim_q \uparrow \sup_{\theta, n<q} \|H_e(2n\pi + \theta) - H_e(2n\pi)\|; \quad 0 \le \theta \le 2\pi$$

where τ denotes the set of trajectories for which the sampled momentum remains bounded, M^0 is the bound on the momentum transfer during any orbit, and H^{01}_{sat} is the absolute saturation limit of the CMG system. The class of momentum management policies considered consists of a large attitude maneuver through angle ε_x about the $\hat{X}_b$-axis followed by an adaptive sequence of small attitude maneuvers through angle ε_y about the displaced $\hat{Y}_b$-axis. The functional form of ε_y is confined to the following class:

$$\begin{aligned}\varepsilon_y(\theta) &= A(\theta)H_{0x}(2n\pi) + B(\theta)H_{0y}(2n\pi) + C(\theta)H_{0z}(2n\pi) \quad \text{for } (2n+1)\pi \le \theta \le 2(n+1)\pi \\ &= 0 \quad \text{for } 2n\pi < \theta < (2n+1)\pi\end{aligned} \tag{2}$$

where $H_0(2n\pi)$ is a linear combination of momentum samples. Comments on modification of the desaturation period are presented in the conclusion.

In Sec II, the first-order perturbation of a circular orbit attitude control law caused by orbital eccentricity is reviewed. The succeeding sections deal with the performance of the aforementioned class of momentum management policies for satellite orbits in the vicinity of that orbit for which the system gains have been chosen. The characteristic equation of the sampled momentum is derived for general momentum sampling (digital controller), switching logic, and system gains. The satellite orbital parameters are assumed arbitrary and in general are in the neighborhood of the design orbit.

The main contribution of this paper is addressed to stability analysis for the following momentum sampling scheme:

$$H_{0j}(2n\pi) = H_j(2n\pi) - H_j(0); \quad j = x, y, z \tag{3}$$

The sampled momentum by the nth orbit is shown to converge to $f + H(0)$ provided $\|K(a, \varepsilon, \theta_p)\|_{op} < 1$. f is the solution of the linear operator equation

$$f - K(a, \varepsilon, \theta_p)f = g(a, \varepsilon, \theta_p) \tag{4}$$

on momentum space, g is the disturbance momentum accumulation per orbit from the gravity gradient torque, and $H(0)$ is the initial stored momentum.

A linear (first order in eccentricity) stability analysis is presented and the results are compared with the exact stability condition for bounded sampled momentum as expressed by Eq. (4). These studies are combined to derive the range of eccentricity for which the sampled momentum remains bounded within H^0_{sat} provided the system gains are chosen with respect to a circular orbit of radius $r_0 = a$, the true mean satellite orbital radius. The study is extended to a neighborhood of orbits without the necessity of measuring the true mean radius.

Throughout, the space vehicle is assumed to move in an inverse square law gravitational field. All perturbations of the orbit are disregarded as well as aerodynamic and solar radiation torques. The pertinent reference system is the ATM reference system (Fig. 1 and Fig. 2) with the $\hat{Z}_R$ axis toward the sun and parallel to the Earth–sun line, the $\hat{X}_R$ axis in the orbital plane and the $\hat{Y}_R$ axis completing the right-hand orthogonal system with terminus in the northern hemisphere. The vehicle reference

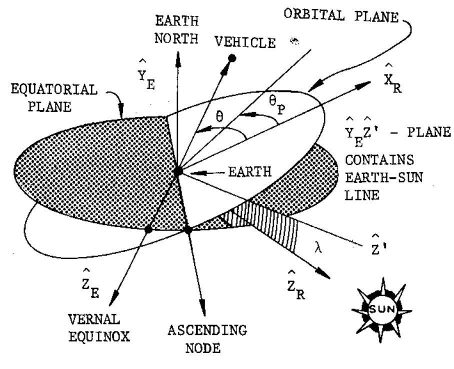

Fig. 1 ATM reference system.

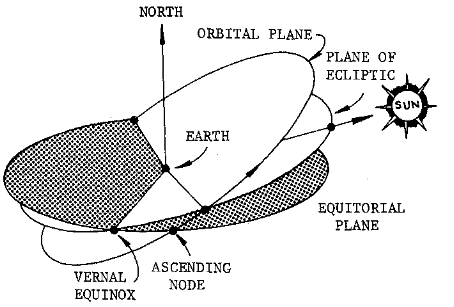

Fig. 2 Celestial sphere.

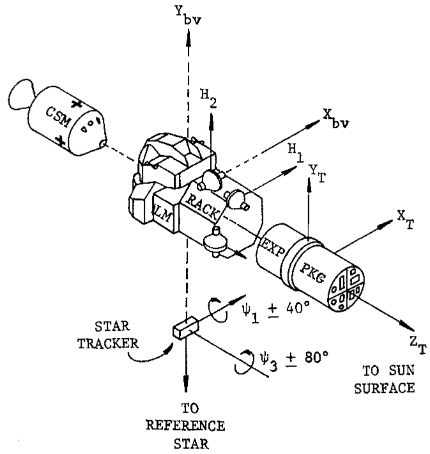

Fig. 3 ATM/LM/CSM cluster configuration and vehicle coordinates.

system (Fig. 3) is oriented parallel to the ATM reference system at $\theta = 0$. Please note that $\hat{X}_v$ will be in the orbital plane; that the solar panels have been omitted; and that $\hat{X}_{bv}$ is parallel to $\hat{X}_v$, $\hat{Y}_{bv}$ is parallel to $\hat{Y}_v$, and $\hat{Z}_{bv}$ is parallel to $\hat{Z}_v$ during the experimental hold mode. Because of Earth orbit and solar rates, these systems are quasi-inertial. This paper is concerned with the inertial period between updates. The principal axes of the satellite inertia tensor, $\hat{X}_b$, $\hat{Y}_b$, $\hat{Z}_b$ coincide respectively, with $\hat{X}_v$, $\hat{Y}_v$, $\hat{Z}_v$ axes during the experimental hold mode. The results of this study are also applicable to the case when the $\hat{Z}_R$ axis is directed toward a reference star in which case updates are conceptually unnecessary.

II. Perturbation Control Functions

The truncated expression for the gravity gradient torque is

$$T_g = (3g_0 R_0^2/2r^3)\hat{r} \times I \cdot \hat{r} \tag{5}$$

Disregarding terms quadratic in the small angle maneuver[15]

$$T_g = M_\theta H_0(2n\pi) + \tilde{\pi} \tag{6}$$

during the desaturation period $[(2n+1)\pi, 2(n+1)\pi]$.

The matrix M_θ can be written as $M_t M_{cf}$ where M_{cf} is diagonal in the control functions A, B, C. M_t depends on the location of the center of mass of the vehicle relative to the center of the earth, the principal components of inertia, the pointing angle, and the large angle maneuver.

Suppose the following constraints are imposed on the control functions 1) at the termination of the desaturation period $[(2n+1)\pi, 2(n+1)\pi]$ the CMGs must accumulate $-[H(2n\pi) - H(0)]$ from the controllable torque component $M_\theta H_0(2n\pi)$ and 2) at the sampling instants there must be zero coupling, i.e., $\int(T_g - \tilde{\pi})\,dt$ is proportional to H_0 where $\int$ denotes integration over $[(2n+1)\pi, 2(n+1)\pi]$.

For the sampling scheme

$$H_0(2n\pi) = H(2n\pi) - H(0) \tag{7}$$

these constraints are summarized by the constraint equation

$$\int M_\theta(dt/d\theta)\,d\theta = -I \tag{8}$$

Restricting the vehicle to a circular orbit of radius r_0, the following attitude control law (5, 6) is a solution to this equation.

$$A_0 = a\,\text{sgn}(\sin 2\theta) \tag{9a}$$

$$B_0 = b[2/\pi + (K_5/K_6)\text{sgn}(\cos 2\theta)] \tag{9b}$$

$$C_0 = c[2/\pi + (K_3/K_4)\text{sgn}(\cos 2\theta)] \tag{9c}$$

where the K_j depend on the large angle maneuver and the pointing angle λ[6,9] the system gains are

$$a = -1/[3\omega_{0c}(I_{xx} - I_{zz})\sin(\varepsilon_x + \lambda)] \tag{10a}$$

$$b = -K_6/[3\omega_{0c}(I_{xx} - I_{zz})\sin 2(\varepsilon_x + \lambda)] \tag{10b}$$

$$c = (K_4/K_6)b \tag{10c}$$

$$\omega_{0c} = (g_0 R_0^2/r_0^3)^{1/2} \tag{10d}$$

If the satellite orbit is slightly eccentric with parameters $(a, \varepsilon, \theta_p)$, the first order perturbation of Eq. (9) can be found in the following manner. The control function solution to the constraint equation is decomposed as follows

$$A = A_0 + A_\varepsilon; \quad B = B_0 + B_\varepsilon; \quad C = C_0 + C_\varepsilon \tag{11}$$

A_0, B_0, C_0 satisfy the constraint equation for a circular orbit of radius $r_0 = a$. The perturbation control functions are

$$A_\varepsilon = a_0 + a_1\,\text{sgn}(\sin 2\theta) + a_2\,\text{sgn}(\sin 3\theta) \tag{12a}$$

$$B_\varepsilon = b_0 + b_1\,\text{sgn}(\cos 2\theta) + b_2\,\text{sgn}(\cos 3\theta) \tag{12b}$$

$$C_\varepsilon = c_0 + c_1\,\text{sgn}(\cos 2\theta) + c_2\,\text{sgn}(\cos 3\theta) \tag{12c}$$

The control functions (11) must satisfy the constraint equation to first-order in eccentricity. Writing the integrand of the constraint equation as

$$(M_0 + M_\varepsilon)(1 + \varepsilon\cos(\theta - \theta_p)) \tag{13}$$

where M_0 contains the circular orbit control functions and M_ε contains the correction terms $A_\varepsilon, B_\varepsilon, C_\varepsilon$ it can be shown[15] that the control functions (11) satisfy the constraint equation to first order in eccentricity if and only if the perturbation control functions satisfy

$$\int M_\varepsilon\,d\theta = -\varepsilon\int M_0\cos(\theta - \theta_p)d\theta \tag{14}$$

a modified constraint equation. Furthermore, the perturbation system gains are uniquely determined[15] if the matrices

$$M_{c0}M_{k1} + M_{c1}M_{k2} + M_{c2}M_{k3}; \quad k = 1, 2, 3 \tag{15}$$

are nonsingular, where

$$M_{c0} \triangleq (\tfrac{3}{2})\omega_{0c}\int M_t'\,d\theta \tag{16}$$

$$M_{c1} \triangleq (\tfrac{3}{2})\omega_{0c}\int M_t'\,\text{diag}[\text{sgn}(\sin 2\theta), \text{sgn}(\cos 2\theta), \text{sgn}(\cos 2\theta)]d\theta$$

$$M_{c2} \triangleq (\tfrac{3}{2})\omega_{0c}\int M_t'\,\text{diag}[\text{sgn}(\sin 3\theta), \text{sgn}(\cos 3\theta), \text{sgn}(\cos 3\theta)]d\theta$$

$$\omega_{0c} = (g_0 R_0^2/a^3)^{1/2}$$

and M_t' satisfies

$$M_\theta = (3g_0 R_0^2/2r^3)M_t' M_{cf} \tag{17}$$

In general, the objective of transferring $[-\Delta H(2n\pi)]$ by the controllable vector momentum to the CMGs at the termination of the $(n+1)$st management period with a zero coupling constraint imposes the demands 1) that for an eccentric orbit the number of small angle maneuvers increases over that required for a circular orbit and 2) that the system gains depend on the orbital parameters.

Because of random errors at orbital insertion, the true orbital parameters $(a, \varepsilon, \theta_p)$ will differ from those of the design circular orbit. Rather than execute a variable gain momentum management scheme which depends on the measurement of the orbital parameters, it is recommended that a minimum maneuver fixed gain policy be implemented. Such a policy must provide stability for neighboring satellite orbits. In particular, the sampled momentum must remain bounded.

III. Sampled Data Approach to Attitude Control Law Stability

Any management policy from the class of momentum management schemes (2) can be mathematically modeled as a feedback control system with a digital controller preceding a linear plant in the feed forward path (Fig. 4 and Fig. 5). The sampled output of the digital controller reflects the momentum sampling scheme. The output is fed into the theta domain product of a zero order hold circuit and a linear system having transition matrix Φ.

$$\Phi(\theta) \triangleq \Phi'(2\pi - \theta) \tag{18}$$

$$\Phi' \triangleq M_\theta(dt/d\theta) \tag{19}$$

The resultant signal is modulated by $f(\cdot)$ and integrated to give the control momentum H_c.

The total vehicle momentum transferred to the CMGs, referred to as the error momentum, is the sum of the control momentum and the disturbance momentum.

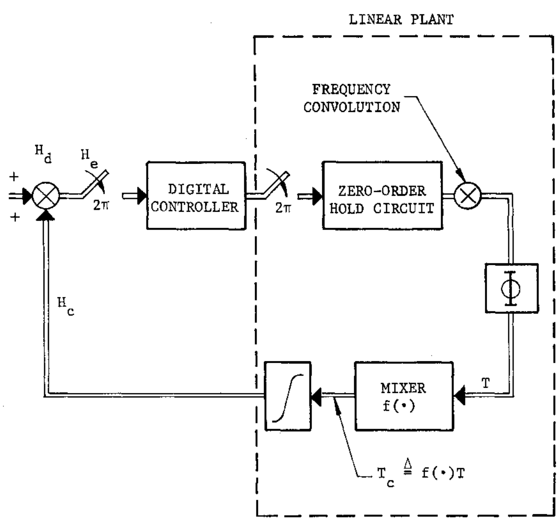

Fig. 4 Mathematical feedback control model. The state transition matrix, Φ, depends on M_θ and $dt/d\theta$. M_θ is chosen for switching logic and system gains independent of the orbital parameters $(a, \varepsilon, \theta_p)$. The linear plant, however, depends on the orbital parameters.

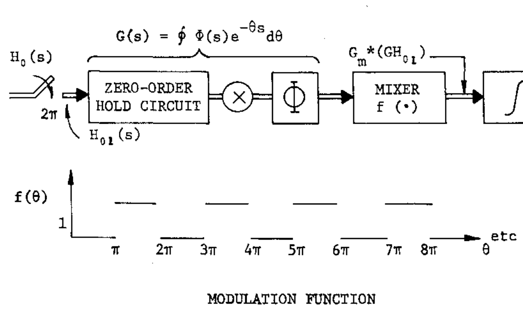

Fig. 5 Linear plant.

The disturbance torque consists of the gravity gradient torque during the experimental hold mode and the uncontrollable torque during the desaturation period.

The response of the linear plant to input $H_0(s)$ is the control momentum

$$H_c(s) = s^{-1}[G_m^*(GH_{01})](s) \tag{20}$$

in the Laplace domain. H_{01} is the Laplace transform of the sampled output of the digital controller.

$$G(s) = \oint \Phi(\theta)e^{-\theta s}\,d\theta \tag{21}$$

and

$$G_m(s) = \int_0^\infty f(\theta)e^{-\theta s}\,ds \tag{22}$$

is the Laplace transform of the modulation function $f(\cdot)$. The state transition matrix, Φ, depends on the control functions (switching logic and system gains) which in turn have been chosen with respect to a particular design orbit. Φ is also functionally dependent on the true orbital parameters $(a, \varepsilon, \theta_p)$.

The z-transform of Eq. (20) is $H_c^*(z)$. Since the linear plant is time-invariant

$$H_c^*(z) = F^*(z)H_0^*(z) \tag{23}$$

where $F^*(z)$ denotes the z-transform of the linear plant. The momentum sampling scheme (3) will be used to derive $F^*(z)$.

The z-transform of the output of the digital controller is

$$H_0^*(z) = [H_e(2\pi) - H_e(0)]z^{-2} + [H_e(4\pi) - H_e(0)]z^{-3} + \cdots$$

$$H_0^*(z) = H_e^*(z) + [-1/(1 - z^{-1})]H_e(0) \tag{24}$$

The error momentum has z-transform

$$\begin{aligned} H_e^*(z) = {} & H_e^*(0) + [H_e(0) + \tilde{g}]z^{-1} \\ & + \{H_e(2\pi) + g + Q[H_e(2\pi) - H_e(0)]\}z^{-2} \\ & + \{H_e(4\pi) + g + Q[H_e(4\pi) - H_e(0)]\}z^{-3} + \cdots \end{aligned} \tag{25}$$

where

$$Q(a, \varepsilon, \theta_p) = \int M_\theta(dt/d\theta)d\theta \tag{26}$$

and $\tilde{g}$ is the disturbance momentum accumulation per orbit for the first orbit during which there are no maneuvers and g is the disturbance momentum accumulation per orbit for all subsequent orbits. $H_e^*(z)$ can also be expressed as

$$\begin{aligned} H_e^*(z) = {} & H_e(0) + [H_e(0) + \tilde{g}]z^{-1} + \{H_e(0) + \tilde{g} + g \\ & + Q[H_e(2\pi) - H_e(0)]\}z^{-2} + \{H_e(0) + \tilde{g} + 2g \\ & + Q[H_e(2\pi) - H_e(0)] + Q[H_e(4\pi) - H_e(0)]\}z^{-3} \\ & + \cdots \end{aligned} \tag{27}$$

But the control momentum is initially zero. Thus, Eq. (27) can be written as

$$\begin{aligned} H_e^*(z) = {} & H_d^*(z) + Q[H_e(2\pi) - H_e(0)]z^{-2} \\ & + \{Q[H_e(2\pi) - H_e(0)] + Q[H_e(4\pi) - H_e(0)]\}z^{-3} + \cdots \end{aligned} \tag{28}$$

Consequently, the z-transform of the linear plant is

$$F^*(z) = z^{-1}/(1 - z^{-1})Q(a, \varepsilon, \theta_p) \tag{29}$$

If higher-order differences are included in the functional form of the small angle maneuver, the sampled output of the digital controller becomes

$$H_0^*(z) = C^*(z)H_e^*(z) + [-1/(1 - z^{-1})]H_e(0) \tag{30}$$

In general,

$$H_e^*(z) = H_d^*(z) + F^*(z)H_0^*(z) \tag{31}$$

Incorporating the previous equations into (31)

$$H_e^*(z) = \{I - z^{-1}[I + Q(a, \varepsilon, \theta_p)C^*(z)]\}^{-1}\{[z^{-1}/(1 - z^{-1})]g + z^{-1}(\tilde{g} - g) + [1/(1 - z^{-1})][I - z^{-1}(I + Q(a, \varepsilon, \theta_p)]H_e(0)\}$$

This equation expresses the z-transform of the sampled momentum as a function of general momentum sampling, switching logic, and system gains. The true orbital parameters $(a, \varepsilon, \theta_p)$ need not coincide with those of the design orbit. The characteristic equation of the sampled momentum is

$$m(z) = \det\{I - z^{-1}[I + Q(a, \varepsilon, \theta_p)C^*(z)]\}$$

The management policy must certainly satisfy the condition that the sampled momentum is nondivergent over the anticipated range of neighboring orbits. The solution of this problem in essence defines an admissible set in the orbital parameter space. Another analytical technique must be developed to choose the orbital parameters from the admissible set for which the sampled momentum remains bounded within the saturation limit H^0_{sat} of the exchange device. The remainder of this paper develops just such a technique for the sampling scheme (3). The switching logic and system gains are arbitrary.

IV. Operator Approach to Stability

A. Convergence of the Sampled Momentum

If the system gains satisfy the following generalized constraint equation

$$(3g_0R_0^2/2r_0C_0)\int M_\theta' \, d\theta = -I \tag{32}$$

the control functions will be said to have been designed for an orbital radius r_0 and center of mass angular momentum C_0. The controllable vector momentum imparted to the CMGs during the desaturation period $[(2n + 1)\pi, 2(n + 1)\pi]$ is

$$(3g_0R_0^2/2)\int \{[1 + \varepsilon\cos(\theta - \theta_p)]/aC(1 - \varepsilon^2)\}M_\theta' \, d\theta \Delta H(2n\pi) \tag{33}$$

for management policies satisfying the generalized constraint equation

$$(3g_0R_0^2/2)\int \{[1 + \varepsilon\cos(\theta - \theta_p)]/aC(1 - \varepsilon^2)\}M_\theta' \, d\theta = +[r_0C_0/aC(1 - \varepsilon^2)][-I + \varepsilon\Delta(r_0, \theta_p)] \tag{34}$$

with

$$\Delta(r_0, \theta_p) = (3g_0R_0^2/2r_0C_0)\int \cos(\theta - \theta_p)M_\theta' \, d\theta \tag{35}$$

Suppose that the system gains are adjusted for a design radius $r_0 = a$, the mean radius, and angular momentum $C_0 = 2\pi a^2/T$, where $T = 2\pi(a^3/g_0R_0^2)^{1/2}$. The operator $Q(a, \varepsilon, \theta_p)$ [see Eq. (26)] equals

$$Q(a, \varepsilon, \theta_p) = -(1 - \varepsilon^2)^{-3/2}I + \varepsilon(1 - \varepsilon^2)^{-3/2}\Delta(a, \theta_p) \tag{36}$$

where

$$\Delta(a, \theta_p) = (\tfrac{3}{2})\omega_{0c}\int \cos(\theta - \theta_p)M_\theta' \, d\theta; \quad \omega_{0c} = (g_0R_0^2/a^3)^{1/2}$$

Sampling the momentum with period 2π yields

$$H_e(2\pi) = H_e(0) + \tilde{g}$$
$$H_e(4\pi) = H_e(2\pi) + g + Q[H_e(2\pi) - H_e(0)]$$
$$H_e[2(n + 1)\pi] = H_e(2n\pi) + g + Q[H_e(2n\pi) - H_e(0)] \tag{37}$$

In general,

$$H_e(2n\pi) = [I + K + K^2 + \cdots + K^{n-1}]g + H_e(0) + K^{n-1}(\tilde{g} - g) \tag{38}$$

where

$$K(a, \varepsilon, \theta_p) = I + Q(a, \varepsilon, \theta_p) \tag{39}$$

If the operator $K(a, \varepsilon, \theta_p)$ satisfies the inequality[16,17]

$$\|K(a, \varepsilon, \theta_p)\|_{op} < 1 \tag{40}$$

then the sequence $[H_e(2n\pi)]$ is Cauchy in momentum space, where the operator norm $\|\cdot\|_{op}$ is defined by

$$\|K(a, \varepsilon, \theta_p)\|_{op} = \sup_\sigma[\|K(a, \varepsilon, \theta_p)x\|] \tag{41}$$

where σ denotes the surface of the unit sphere in M. Since momentum space M is a Banach space there exists a vector f in M such that the Neumann series

$$g + Kg + K^2g + \cdots \tag{42}$$

converges in norm to the vector f. By the complete continuity of $K(a, \varepsilon, \theta_p)$, f satisfies the equation

$$f - K(a, \varepsilon, \theta_p)f = g(a, \varepsilon, \theta_p) \tag{43}$$

B. Linear Stability Analysis

Neglecting higher-order terms in eccentricity the linear operator $K(a, \varepsilon, \theta_p)$ becomes

$$K(a, \varepsilon, \theta_p) = \varepsilon\Delta(a, \theta_p) \tag{44}$$

The sampled error momentum by the nth orbit is

$$H_e(2n\pi) = [I + \varepsilon\Delta + \cdots + \varepsilon^{n-1}\Delta^{n-1}]g + H_e(0) + \varepsilon^{n-1}\Delta^{n-1}(\tilde{g} - g) \tag{45}$$

For all eccentricity less than

$$\varepsilon_{max} = 1/\sup_{\theta_p}\|\Delta(a, \theta_p)\|_{op} \tag{46}$$

the sampled error momentum in Eq. (45) remains bounded for arbitrary angular position of perigee. $H_e(2n\pi)$ converges in norm to $f_0 + H_e(0)$ where f_0 solves the equation

$$f_0 - \varepsilon\Delta(a, \theta_p)f_0 = g(a, \varepsilon, \theta_p) \tag{47}$$

Because of the error in the linear analysis there is a correction vector c such that

$$f = f_0 + c \tag{48}$$

where f solves Eq. (43). The correction vector equals

$$c = (I - \varepsilon\Delta)^{-1}(K - \varepsilon\Delta)f \tag{49}$$

Substituting the expression for $K(a, \varepsilon, \theta_p)$

$$c = (1 - (1 - \varepsilon^2)^{-3/2})f \tag{50}$$

and

$$f_0 = (1 - \varepsilon^2)^{-3/2}f \tag{51}$$

The linear operator $Q(a, \varepsilon, \theta_p)$ can be expressed as

$$Q(a, \varepsilon, \theta_p) = -[1 + R(\varepsilon)][I - \varepsilon\Delta(a, \theta_p)] \tag{52}$$

where $R(\varepsilon)$ is a non-negative monotone nondecreasing function of the orbital eccentricity. Consequently, for $\varepsilon = 1/\|\Delta(a, \theta_p)\|_{op}$ the operator norm of $K(a, \varepsilon, \theta_p)$ is at least one. Thus, it is impossible to conclude whether or not the Neumann series (42) converges or diverges. A sufficient condition for convergence of the series (40) for $0 \le \varepsilon \le \varepsilon_0$ is

$$R(\varepsilon_0) + \varepsilon[1 + R(\varepsilon_0)]\|\Delta\|_{op} < 1 \tag{53}$$

Thus, the sampled error momentum converges for $\varepsilon < R_{01}$ where

$$R_{01} = \sup_{\varepsilon > 0}\min\{\varepsilon, (1/\|\Delta\|_{op})[1 - R(\varepsilon)]/[1 + R(\varepsilon)]\} \tag{54}$$

For unknown angular position of perigee, the sampled error momentum converges for $\varepsilon < R_0$ where

$$R_0 = \sup_{\varepsilon > 0} \min\{\varepsilon, (1/\sup_{\theta_p}\|\Delta\|_{op})[1 - R(\varepsilon)]/[1 + R(\varepsilon)]\} \quad (55)$$

this certainty bound is slightly less than that given by the linear analysis.

C. Error Momentum within the Saturation Limit

The range of orbital eccentricity for which the sampled error momentum remains bounded is (o, R_o). In addition to the boundedness of $H_e(2n\pi)$, one is also interested in restricting the norm of the error momentum $\|H_e(\theta)\|$ to within the absolute saturation limit, H_{sat}^{01}, of the CMG system. This is equivalent to the constraint

$$\|H_e(2n\pi)\| < H_{sat}^{0} \ \forall\, n \quad (56)$$

where

$$H_{sat}^{0} = H_{sat}^{01} - (1 - \alpha)^{-1}M^0, \quad 0 < \alpha < 1 \quad (57)$$

and

$$M^0 = \sup_{\tau} \lim_{q} \uparrow \sup_{\theta, n<q} \|H_e(2n\pi + \theta) - H_e(2n\pi)\| \quad (58)$$

τ denotes the set of trajectories

$$\tau = \{(a, \varepsilon, \theta_p); \quad 0 \le \theta_p \le 2\pi, \quad 0 \le \varepsilon < R_0\} \quad (59)$$

and α is a safety factor.

The system constraint Eq. (56) will modify the certainty bound R_0. The derivation is as follows: Let

$$H_{sat} = H_{sat}^{0} - \sup_{\tau, m>1} \|H_e(0) + K^{m-1}\tilde{g}\| \quad (60)$$

Then, $\|f\| < (\frac{1}{2})H_{sat}$ implies that at each sampling instant

$$\|H_e(2n\pi)\| < H_{sat}^{0}$$

From the linear analysis

$$\|f\| \le \|f_0\| \le \|g\|/(1 - \varepsilon \sup_{\theta_p}\|\Delta\|_{op}) \quad (61)$$

for $\varepsilon < 1/\sup_{\theta_p}\|\Delta\|_{op}$. Consequently, the constraint

$$\|g(a, \varepsilon, \theta_p)\|/(1 - \varepsilon \sup_{\theta_p}\|\Delta\|_{op}) < (\tfrac{1}{2})H_{sat} \quad (62)$$

implies Eq. (56). Recall that g is the disturbance momentum accumulation per orbit and depends on the true orbital parameters and the control law. Let $\|g\|_{a(1-\varepsilon)}$ denote the norm of the disturbance momentum accumulation per orbit for the same control law and for a circular orbit of radius $a(1 - \varepsilon)$. The sampled error momentum is bounded for $\varepsilon < R_0 < 1/\sup_{\theta_p}\|\Delta(a, \theta_p)\|_{op}$. Let

$\varepsilon_0 = 1/\sup_{\theta_p}\|\Delta(a, \theta_p)\|_{op}$.

Then

$$\sup_{\tau}\|g(a, \varepsilon, \theta_p)\| \le \|g\|_{a(1-\varepsilon_0)} \quad (63)$$

Thus, $H_e(2n\pi)$ remains not only bounded but within the saturation limit, H_{sat}^{0}, for $\varepsilon < R_{01}$ and arbitrary angular position of perigee, where

$$R_{01} = \min\{R_0, (1 - 2\|g\|_{a(1-\varepsilon_0)}/H_{sat})/\sup_{\theta_p}\|\Delta\|_{op}\} \quad (64)$$

D. Extension of Results

Results of the previous paragraphs are not completely dependent on the knowledge of the true mean radius a of the satellite orbit. Suppose the system gains satisfy the generalized constraint equation

$$(3g_0R_0^2/2r_0C_0)\int M_\theta'\, d\theta = -I \quad (65)$$

The center of mass angular momentum for an orbit having parameters $(a, \varepsilon, \theta_p)$ is

$$C = [\mu a(1 - \varepsilon^2)]^{1/2} \quad (66)$$

where

$$\mu = G(M_e + M_v) \quad (67)$$

G is the gravitational constant, M_e is the mass of the Earth and M_v is the mass of the orbiting vehicle. If the system gains are adjusted for a design radius r_0 and angular momentum $(\mu r_0)^{1/2}$ the operator $Q(a, \varepsilon, \theta_p)$ has the analytic form

$$Q(a, \varepsilon, \theta_p) = -(r_0/a)^{3/2}[1 + R(\varepsilon)][I - \varepsilon\Delta(r_0, \theta_p)] \quad (68)$$

where

$$(1 - \varepsilon^2)^{-3/2} = 1 + R(\varepsilon) \quad (69)$$

The sequence of momentum samples $H_e(2n\pi)$ is Cauchy in momentum space if

$$\|K(a, \varepsilon, \theta_p)\|_{op} < 1 \quad (70)$$

The operator $K(a, \varepsilon, \theta_p)$ is defined by Eq. (39). Consequently,

$$K(a, \varepsilon, \theta_p) = (1 - (r_0/a)^{3/2})I - (r_0/a)^{3/2}R(\varepsilon)I + (r_0/a)^{3/2}\varepsilon[1 + R(\varepsilon)]\Delta(r_0, \theta_p) \quad (71)$$

Taking the operator norm of the right side of Eq. (71) and using the triangle inequality yields

$$\|K(a, \varepsilon, \theta_p)\|_{op} \le [1 - (r_0/a)^{3/2}] + (r_0/a)^{3/2}R(\varepsilon) + (r_0/a)^{3/2}\varepsilon[1 + R(\varepsilon)]\|\Delta\|_{op} \quad (72)$$

Thus, the sequency of momentum samples is Cauchy for arbitrary mean radius and arbitrary angular position of perigee if the eccentricity satisfies

$$R(\varepsilon) + \varepsilon[1 + R(\varepsilon)]\sup_{\theta_p}\|\Delta\|_{op} < 1 \quad (73)$$

Since momentum space is a Banach space and the operator $K(a, \varepsilon, \theta_p)$ is completely continuous (any bounded operator on a finite dimensional space is completely continuous), the sampled momentum converges in norm to $f + H_e(0)$ where the vector f satisfies the equation

$$f - K(a, \varepsilon, \theta_p)f = g(a, \varepsilon, \theta_p) \quad (74)$$

$H_e(0)$ is the initial stored momentum and $g(a, \varepsilon, \theta_p)$ is the disturbance momentum accumulation per orbit. The sampled momentum converges for unknown mean radius, unknown angular position of perigee and all eccentricity $\varepsilon < R_0$. Equation (55) defines the certainty bound R_0. R_0 is the value of eccentricity at the intersection of the two functions

$$f_1(\varepsilon) = \varepsilon \quad (75)$$

and

$$f_2(\varepsilon) = (1/\sup_{\theta_p}\|\Delta\|_{op})[1 - R(\varepsilon)]/[1 + R(\varepsilon)] \quad (76)$$

Recall that $R(\varepsilon)$ is a non-negative monotone nondecreasing function of the orbital eccentricity. Also,

$$R(0) = 0$$

Thus, the certainty bound R_0 is greater than zero.

To maintain fine attitude control during the daylight orbital sector throughout the mission, the constraint Eq. (56) must be satisfied. The set of trajectories τ for which the sampled momentum remains bounded is

$$\tau = \{(a, \varepsilon, \theta_p); \quad 0 \le \theta_p \le 2\pi, \quad 0 \le \varepsilon < R_0, \quad \text{arbitrary } a\} \quad (77)$$

This set includes satellite orbits which are not in the neighborhood of the design orbit. The mean radius will, in reality, fall in some tolerance band β about the design radius r_0. Momentum management scheme stability in the sense of maintaining fine attitude control is analytically defined by Eqs. (56–58). A complete set of neighboring satellite orbits is defined by

$$\tau = \{(a, \varepsilon, \theta_p);\quad 0 \leq \theta_p \leq 2\pi,\quad 0 \leq \varepsilon < R_0,\quad a \text{ in } \beta\} \tag{78}$$

But the set of trajectories for which the sampled momentum remains bounded certainly contains the set of neighboring trajectories.

Using paragraph B as a guide it is easily shown that there exists a neighborhood η of orbits in the vicinity of the design orbit for which fine attitude control is maintained. Let f_0 denote the vector solution of the equation

$$f_0 - \varepsilon\Delta(r_0, \theta_p)f_0 = g(a, \varepsilon, \theta_p) \tag{79}$$

Consequently,

$$f_0 = (I - \varepsilon\Delta)^{-1}(I - K)f \tag{80}$$

and

$$\|f\| < (a/r_0)^{3/2}\|f_0\| \tag{81}$$

Thus, $H_e(2n\pi)$ remains not only bounded but within the saturation limit, H^0_{sat}, for $\varepsilon < R_{01}$, mean radius in the tolerance band β about r_0 and arbitrary angular position of perigee, where

$$R_{01} = \min\{R_0, [1 - 2\sup_{\tau}(a/r_0)^{3/2}\|g\|/H_{\text{sat}}]/\sup_{\theta_p}\|\Delta\|_{\text{op}}\} \tag{82}$$

M^0, however, is the bound on the total variation of the CMG momentum over any 2π orbital sector and for any neighboring orbit in τ for which the momentum remains bounded. Consequently, the continuous time CMG momentum history remains within the absolute saturation limit.

V. Conclusion

In practice, command rates are initiated about the body fixed vehicle axes. This vehicle reference system is illustrated in Fig. 3 and is a body fixed orthogonal triad. If the principal axes of the vehicle inertia tensor are misaligned with respect to the body fixed vehicle system, the representation of M_θ with respect to the vehicle system must reflect the unknown misalignment error in parametric form. The torque, however, is still expressed as

$$T_g = M_\theta H(2n\pi) + \tilde{\pi} \tag{83}$$

during the desaturation period $[(2n + 1)\pi, 2(n + 1)\pi]$.

The desaturation period need not extend over a π radian orbital sector. The modulation function need only be appropriately modified. $Q(a, \varepsilon, \theta_p)$ in Eq. (26) becomes

$$Q(a, \varepsilon, \theta_p) = \int_\chi M_\theta(dt/d\theta)d\theta \tag{84}$$

where χ denotes the desaturation sector symmetric about the midnight terminator.

The generalized constraint equation is

$$(3g_0R_0^2/2r_0C_0)\int_\chi M'_\theta\, d\theta = -I \tag{85}$$

and

$$\Delta(r_0, \theta_p) = (3g_0R_0^2/2r_0C_0)\int_\chi \cos(\theta - \theta_p)M'_\theta\, d\theta \tag{86}$$

The sampled data approach to attitude control law stability over neighboring orbits provides the analyst complete freedom to choose the momentum sampling scheme (digital controller), maneuver times (switching logic) and system gains. The equation for the sampled momentum has been derived for arbitrary satellite orbital parameters.

Using an operator approach to stability, the problem of sustaining a $2\pi - \chi$ orbital sector of fine attitude control over neighboring orbits throughout the mission and for the sampling scheme

$$H_{0j}(2n\pi) = H_j(2n\pi) - H_j(0);\quad j = x, y, z$$

has been solved. The solution is general in the sense that the analyst has complete freedom to choose the maneuver profile and system gains consistent with the generalized constraint equation.

References

[1] Chubb, W. B., Schultz, D. N., and Seltzer, S. M., "Attitude Control and Precision Pointing of the Apollo Telescope Mount," AIAA Paper 67-534, Huntsville, Ala., 1967.

[2] O'Conner, B. J. and Marine, L. A., "A Description of the CMG and Its Application to Space Vehicle Control," *Journal of Spacecraft and Rockets*, Vol. 6, No. 3, March 1969, pp. 225–231.

[3] Greenberg, M., "A Gravity Gradient Desaturation Scheme for the LM/ATM Mission," Eng. File MT-15248, Dec. 1967, The Bendix Corp., Teterboro, N.J.

[4] Shea, J. P., "Sample Data Momentum Desaturation for the ATM Cluster," Eng. File MT-15248, Dec. 1967, The Bendix Corp., Teterboro, N.J.

[5] Rybak, C., "Gravity Gradient Momentum Dump of the CSM/LM/ATM Vehicle Configuration," Eng. File MT-1617, Feb. 1968, The Bendix Corp., Denver, Colo.

[6] MacLennan, W. D., "The Momentum Management Problem," BD-2148, June 1968, Bendix Research Labs., Southfield, Mich.

[7] Kennel, Hans F., "Angular Momentum Desaturation for ATM Cluster Configuration Using Gravity Gradient Torques," TM X-53748, May 1968, NASA.

[8] Frik, Martin A., "Desaturation of the ATMs Control System By Gravity Gradient Torques," TM X-53783, Aug. 1968, NASA.

[9] Kennel, H. F., "Angular Momentum Desaturation for ATM/LM/CSM Configuration Using Gravity Gradient Torques," TM X-53764, Aug. 1968, NASA.

[10] Greenberg, M. S., "Momentum Management Systems," *Bendix Technical Journal*, Vol. 1, No. 1, Spring 1968.

[11] Powell, B. K., "A Momentum Desaturation Law for the CSM/LM/ATM Employing Complex Multiaxis Maneuvers," 3628-3400-69-16, Jan. 1969, Bendix Research Labs., Southfield, Mich.

[12] Kennel, H. F., "Large Angle Method for Space Vehicle Angular Momentum Desaturation Using Gravity Torques," TM X-53958, Oct. 1969, NASA.

[13] Powell, B. K., "Gravity Gradient Desaturation of A Momentum Exchange Attitude Control System," AIAA Paper 71-940, Hofstra Univ., Hempstead, New York, 1971.

[14] Ross, Charles H. and Worley, Dr. Eugene, "Optimized Momentum and Attitude Control System (MACS) for Skylab," AIAA Paper 71-938, Hofstra Univ., Hempstead, New York, 1971.

[15] Mayo, Ronald A., "Orbital Eccentricity and Angular Momentum Gravity Gradient CMG Desaturation Scheme Stability," Eng. File MT-2032, July 1969, The Bendix Corp., Denver, Colo.

[16] Halmos, Paul R., *Finite-Dimensional Vector Spaces*, D. Van Nostrand, New York, 1958.

[17] Friedman, Bernard, *Principles and Techniques of Applied Mathematics*, Wiley, New York, 1956.